Biochimica et Biophysica Acta 1783 (2008) 1707–1717

Contents lists available at ScienceDirect

Biochimica et Biophysica Acta

journal homepage: www.elsevier.com/locate/bbamcr

The optimized allotopic expression of *ND1* or *ND4* genes restores respiratory chain complex I activity in fibroblasts harboring mutations in these genes

Crystel Bonnet [a,1], Sébastien Augustin [a,1], Sami Ellouze [a], Paule Bénit [c,2], Aicha Bouaita [a], Pierre Rustin [c,2], José-Alain Sahel [a,b], Marisol Corral-Debrinski [a,*]

[a] Institut de la Vision, Université Pierre et Marie Curie-Paris, INSERM UMR-S 592, 17 rue Moreau, Paris, F-75012 France
[b] Centre Hospitalier National d'Ophtalmologie des Quinze-Vingts, Service 4, 28 rue de Charenton, Paris, F-75012 France
[c] INSERM U676, Hôpital Robert Debré 48, Bd Sérurier 75019 Paris, France

ARTICLE INFO

Article history:
Received 4 December 2007
Received in revised form 5 March 2008
Accepted 22 April 2008
Available online 6 May 2008

Keywords:
Complex I and V activities
Nuclearly-encoded ND1 and ND4 genes
Oxidative phosphorylation
LHON

ABSTRACT

Leber's Hereditary Optic Neuropathy (LHON) was the first maternally inherited mitochondrial disease identified and is now considered the most prevalent mitochondrial disorder. LHON patients harbor mutations in mitochondrial DNA (mtDNA). In about 90% of cases, the genes involved encode proteins of the respiratory chain complex I. Even though the molecular bases are known since 20 years almost all remains to be done regarding physiopathology and therapy. In this study, we report a severe decrease of complex I activity in cultured skin fibroblasts isolated from two LHON patients harboring mutations in *ND4* or *ND1* genes. Most importantly, we were able to restore sustainably (a) the ability to grow on galactose, (b) the ATP synthesis rate and (c) the complex I activity, initially impaired in these cells. Our strategy consisted of forcing mRNAs from nuclearly-encoded *ND1* and *ND4* genes to localize to the mitochondrial surface. The rescue of the respiratory chain defect observed was possible by discreet amounts of hybrid mRNAs and fusion proteins demonstrating the efficiency of their mitochondrial import. Hence, we confirmed here for two mitochondrial genes located in the organelle that the optimized allotopic expression approach represents a powerful tool that could ultimately be applied in human therapy for LHON.

1. Introduction

Leber's Hereditary Optic Neuropathy (LHON) is a maternally inherited neurodegenerative disorder, recognized as the most frequently occurring mitochondrial disease [1]. The pathology is due to point mutations in the mitochondrial genome. The three most common pathogenic mutations found in about 90% of LHON's patients are located in *ND1* (G3460A), *ND4* (G11778A) or *ND6* (T14484C) genes. They encode subunits of the respiratory chain complex I and the mutations have the double effect of lowering ATP synthesis and increasing oxidative stress chronically. The pathology is characterized by selective death of retinal ganglion cells and optic nerve atrophy, prevalently in young males leading to irreversible visual failure [2]. Since the discovery in 1988 of the deleterious nucleotide substitution G11778A in the *ND4* gene [3] and thereafter the mutations in *ND1* [4] and *ND6* [5] genes, the pathogenesis of LHON remains poorly understood. One hypothesis to explain complex I dysfunction on LHON patients underlies on the defective mitochondrial distribution along the optic nerve head due to the abnormal organelle recruitment and their axonal transport. This would constitute the first step of a vicious event cycle that further compromises cell respiration which eventually lead to profound energy depletion, increased production of reactive oxygen species (ROS) and neuronal cell death through apoptosis [6,7]. Besides, perturbations of the respiratory chain function due to LHON mutations have been very complex to evidence. Biochemical studies in patient-derived tissues and cellular experimental models have produced conflicting results regarding the extent of respiratory chain dysfunction associated with the disease [8,9]. The 3460/*ND1* mutation induced a severe defect of complex I activity in mitochondria from platelets, lymphoblasts and muscle while 11778/*ND4* and 14484/*ND6* mutations are noticeably less severe [10–13]. Moreover, the *ND4*/G11778A mutation, found in 50 to 70% of patients, is associated to an increased resistance to rotenone [14], a classical inhibitor of complex I. Accordingly, the electron transfer through complex I is altered in cybrid cell lines harboring LHON mutations [15–19]. A conformational modification of complex I structure may lead to an increased production of ROS [20]. Indeed, it has been shown that, while mitochondria represent the major intracellular source of ROS, most of the superoxide radicals are produced at complex I in brain mitochondria [21]. Another study has demonstrated an induction of apoptosis in LHON patients due to oxidative stress [22], possibly associated with a decrease in antioxidant defences [23]. Finally, a recent report suggests that in primary retinal cultures glutamate

* Corresponding author. Tel.: +33 1 53 46 25 61; fax: +33 1 53 46 25 02.
E-mail address: marisol.corral@inserm.fr (M. Corral-Debrinski).
[1] These authors contributed equally to this work.
[2] Tel.: +33 1 40 03 19 89; fax: +33 1 40 03 19 78.

0167-4889/$ – see front matter © 2008 Elsevier B.V. All rights reserved.
doi:10.1016/j.bbamcr.2008.04.018

Table 1
RT-PCR analyses

mRNA	RT-PCR product length (pb)	Primers		RT-PCR	
		5′ primer (5′–3′)	3′ primer (5′–3′)	Quantity (ng)	Cycle numbers
Endogenous *ND1*	252	ATACCCATGGCCAACCTCCTACTCCTC	GTTGGGTATGGGGAGGGGGGTTCATAG	50	25
Hybrid *ND1*	248	T3 (AATTAACCCTCACTAAAGGG)	CAGTCAGCATGAGGAAGGCCATGG	300	35
Endogenous *ND4*	227	ATGCTAAAACTAATCGTCCCAACAATT	ATAAGTGGCGTTGGCTTGCCATGATTG	50	25
Hybrid *ND4*	330	T3 (AATTAACCCTCACTAAAGGG)	CAGGAGAACAGGTTGTTGTTGATCTGG	300	35
Endogenous *ATP6*	248	ATGAACGAAAATCTGTTGCTTCATTC	GAGTCCGAGGAGGTTAGTTGTGGCAAT	50	25

RT-PCRs were performed three times using two independent RNA preparations from LHON fibroblasts and theirs counterparts allotopically expressing wild-type genes.

toxicity resulting from impaired glutamate transport may play a role in the pathogenic process of LHON [24]. The many unanswered questions that remain about the disease's molecular pathogenesis hamper devising appropriate therapeutic strategies. Several trials with vitamins or idebenone (an oxygen radical scavenger) were performed, however no evidence to date supports their use and prevention of vision loss in patients [25]. Thus, allotopic expression (expression of mitochondrial genes transferred to the nucleus) of some of mtDNA genes has been tried in cybrid cells harboring deleterious mtDNA mutations as a possible therapeutic option to cure LHON. In 2002, two laboratories reported improvements in oxidative phosphorylation (OXPHOS) function when allotopic expression was used as strategy in cybrid cells harboring mutations in the mitochondrial *ND4* and *ATP6* genes [26,27]. However, several attempts failed to confirm these data and to obtain a complete and long-lasting rescue of the mitochondrial defect *ex vivo* [28,29]. Probably, the highly hydrophobic nature of proteins encoded by the mitochondrial genome represents a physical impediment to mitochondrial import of the allotopically expressed proteins [30]. This strongly limited the potentiality of allotopic expression as a therapeutic approach for mtDNA-related diseases [25,31].

In a recent work we reported in fibroblasts harboring the G11778A *ND4* mutation an incapacity to grow in galactose and a significant decrease in their ability to synthesize ATP *ex vivo*. The optimized allotopic expression of the engineered nucleus-localized wild-type *ND4* gene rescued their inability to grow in galactose and restore a normal rate of ATP synthesis *in vitro* [32]. Our approach has consisted of maximizing the positive effect on mitochondrial function by the sorting of the *ND4* mRNA to the mitochondrial surface, thus ensuring the mitochondrial translocation of the corresponding polypeptide. The specific subcellular transport of the hybrid mRNA was achieved by the generation of an expression vector in which the engineered *ND4* gene was combined with the mRNA *cis*-acting elements of the *COX10* gene, since *COX10* mRNA localizes exclusively to the mitochondrial surface in HeLa cells [33].

In the present study, we examined human cultured skin fibroblasts from LHON patients carrying either the *ND4*/G11778A mutation or the *ND1*/G3460A mutation and their counterparts allotopically expressing nuclear recoded *ND4* or *ND1* wild-type genes. Mitochondrial function in these cells was assessed according to three criteria: growth capacity in galactose medium, ATP synthesis rate and complex I activity. We observed in LHON fibroblasts a severe decrease in complex I activity, i.e. 60% and 80% for *ND4* and *ND1* mutations respectively. Moreover, we demonstrated the presence of hybrid mRNAs and their corresponding proteins in fibroblasts stably expressing our vectors of optimized allotopic expression. When the three criteria of mitochondrial function were monitored in these cells, we observed a significant restoration of OXPHOS function. In fibroblasts bearing the *ND1* mutation, the optimized allotopic expression vector led to an increase of approximately 1.8-fold in the overall amount of ND1 protein, this increase appeared to be sufficient for salvaging OXPHOS in these cells. Hence, our approach for the mitochondrial *ND1* and *ND4* genes ensures the efficient mitochondrial translocation of the corresponding precursors. The rescue of the OXPHOS defect, without observable deleterious consequences for cell fitness, suggested that the processed polypeptides were functional within their respective respiratory chain complexes and, therefore, able to compensate for the endogenous defective proteins.

2. Materials and methods

2.1. Plasmid construction

The construct directing the synthesis of the nuclear version of the *ND4* gene, namely *COX10*^{MTS}*ND4-3′UTR*^{COX10} (*WT-ND4*), was obtained as previously described [32].

The mitochondrial *ND1* sequence was purchased from Genscript Corp. (Piscataway, NJ, USA). The *ND1* ORF of 954 nucleotides (318 amino acids) was recoded for the 22 non-universal codons and optimized to achieve a high-level expression in human cells. At the N-terminal extremity of the protein, it has been added in frame the first 28 amino acids of the human *COX10* gene coding for its mitochondrial targeting sequence (MTS) and 7 additional amino acids, to ensure the MTS cleavage by a mitochondrial processing peptidase (MAASPHTLSSRLLTGCVGGSVWYLERRT). The *COX10*^{MTS}*ND1-3′UTR*^{COX10} construct (*WT-ND1*) was obtained according to the methodology previously described for the *COX10*^{MTS}*ND4-3′UTR*^{COX10} plasmid [32]. Final constructs were entirely sequenced (Genome Express, France) to confirm accuracy of the *COX10* MTS-*ND1* ORF and the *COX10* 3′UTR sequences within the *pCMV-Tag 4A* vector (Stratagene, La Jolla, CA).

2.2. Cell culture and transfection

Cultured skin fibroblasts were derived from forearm biopsies of a healthy subject (15-month-old), a 18-year-old man who carries the G11778A mutation in the *ND4* gene (LHON #1) and a 20-year-old man carrying the LHON *ND1* G3460A (LHON #2). In both LHON patient's fibroblasts, the pathogenic mtDNA mutation was found homoplasmic (all mtDNA molecules were mutated). Fibroblasts were grown under standard conditions in DMEM-Glucose medium (Gibco, Invitrogen) supplemented with 12% fetal bovine serum (Gibco, Invitrogen), Hepes (10 mM), uridine (2.25 mM), gentamicin (10 μg/ml), sodium pyruvate (2 mM) and glutamine (2 mM). About one half million LHON fibroblasts (80,000 per well) were seeded in 6-well plates (approximately 70% of confluence). 24 h later they were transfected with FuGENE 6 transfection reagent as recommended by the manufacturer (Roche Biochemicals, Indianapolis). The selection was performed 68 h later with 0.15 mg/ml of G418 (Roche Biochemicals, Indianapolis) added to the medium, which has been changed each other day. 11 days after the selection, approximately 100,000 cells were counted using a Malassez plate after trypsination of the whole 6-well plates. We estimated the transfection yield of around 25% (number of cells collected after 11 days of G418 selection as compared to the total amount of cells initially seeded for the transfection). However this value would decrease if the number of passages in culture of the recipient cells is higher than 6. After trypsination, cells were seeded in the absence of G418 for 48 h. Thereafter stable clones were expanded for 3 additional weeks in the presence of G418. After each trypsination, 20% of the cells were conserved (liquid nitrogen), the others were used for mitochondrial function evaluation. 36 h before each evaluation the G418 was withdrawn from the medium. In our experience, control or untransfected fibroblasts as well as stably transfected cells cannot be monitored rigorously after their 12th–16th passage in culture.

2.3. Glucose/galactose assay

To determine cell ability to grow in galactose medium immediately after the transfection, 1500 fibroblasts from LHON #2 per well were seeded in two 24-well plates. Transfections were performed 24 h later using either the *COX10*^{MTS}*ND1-3′UTR*^{COX10} or the *pCMV-Tag 4A* vectors. After 68 h, the cells were washed three times with a DMEM medium lacking glucose. Plates were incubated in glucose (25 mM)- or galactose (10 mM)-containing DMEM medium (Gibco, Invitrogen) supplemented with 12% fetal bovine serum (Gibco, Invitrogen), Hepes (10 mM), uridine (2.25 mM), gentamicin (10 μg/ml), sodium pyruvate (2 mM), and glutamine (2 mM). The cells were then cultured for 10 days in the presence of 0.15 mg/ml G418. The medium was renewed every 2 days. At 5 and 10 days, cells were trypsinized and counted with Malassez plates to compare the amount of viable cells under each condition. In parallel, the ability of control fibroblasts to grow in either glucose or galactose media was assessed.

The capacity to grow in galactose medium of stably transfected cells was also compared to control fibroblasts. Fibroblasts stably transfected with either the

COX10^{MTS}*ND1-3′UTR*^{COX10} or the *pCMV-Tag 4A* vectors were maintained for 3 days in a glucose-containing medium lacking G418. After trypsination, 1500 of each transfected cells and control fibroblasts were seeded per well into two 24-well plates. The next day, one of the plates was extensively washed with a medium lacking glucose before the galactose-containing medium was added. The cells were cultured for 14 days, the medium of each plate was changed every 2 days. The number of viable cells was determined, with Malassez plates, after 14 days of growth in either glucose- or galactose-containing media.

2.4. Immunocytochemistry

Immunochemistry was performed using either the mouse monoclonal anti-Flag M2 (Sigma, St. Louis, MO) or anti-ATP synthase α-subunit (Molecular Probes, Invitrogen) antibodies, as previously described [32,34]. The membrane potential-dependent probe MitoTracker Red CMXRos (MT) was obtained from Molecular Probes (Invitrogen) and used as recommended by the manufacturer. Briefly, coverslips with approximately 2000 cells in a 24-well plate were grown for 36 h. Subsequently, the DMEM medium was removed and prewarmed medium containing 10 nM of the dye was added to the cells. They were incubated for 30 min under growing conditions. After the staining, cells were fixed in 3.7% formaldehyde for 15 min before proceeding to the labeling with appropriate antibodies.

Fluorescence was observed using a Leica DM 5000 B Digital Microscope to evaluate the subcellular distribution of the allotopically expressed polypeptides and their possible colocalization with the endogenous ATP synthase α-subunit or with the fluorescent dye MitoTracker. The digital images were acquired and processed with the MetaVue imaging system software.

2.5. RNA extraction, RT-PCR analyses

RNAs from untransfected and transfected fibroblasts were obtained using RNeasy Protect Mini kit (QIAGEN), 2×10^6 cells were required for each RNA preparation. RT-PCR analyses were performed with the Superscript III one step RT-PCR Platinium Taq kit (Invitrogen). Table 1 shows the specific couple of primers used for each gene examined, the expected sizes of the PCR products, the quantity of RNA used for reverse transcription, and the number of PCR cycles performed.

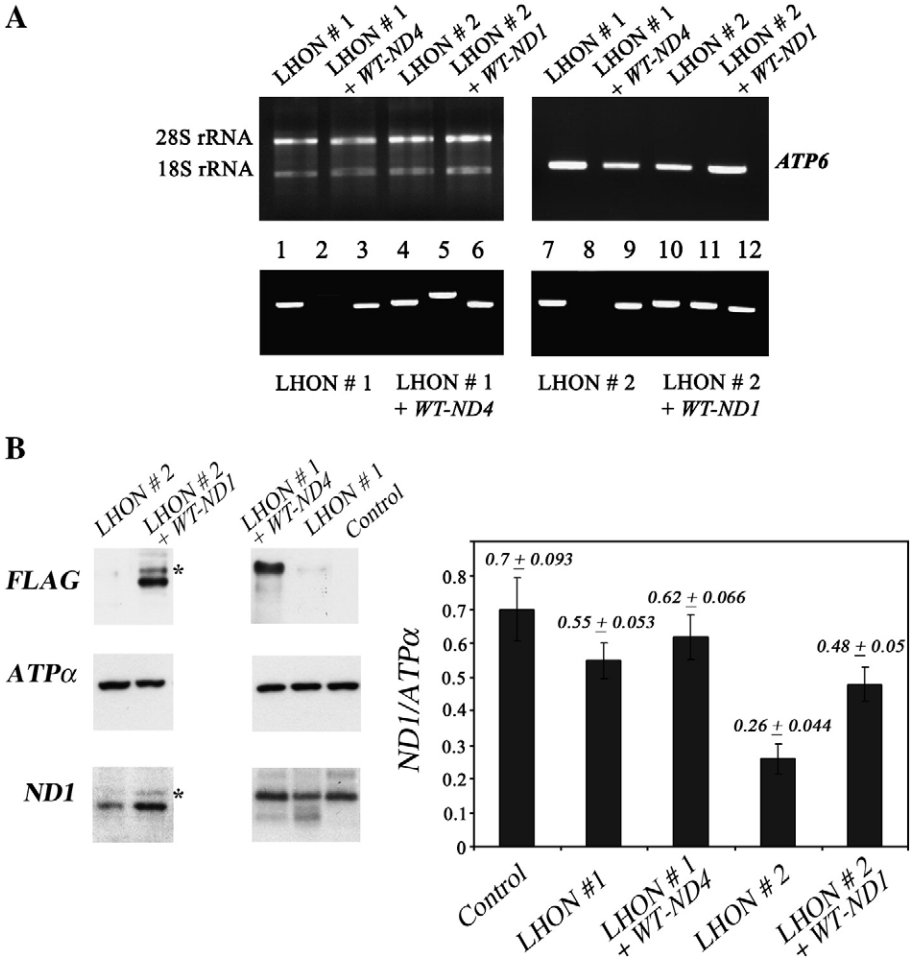

Fig. 1. Steady-state levels of endogenous and hybrid mRNAs from the *ND4* and *ND1* genes, and of the fusion ND4 and ND1 proteins in stably transfected LHON fibroblasts. A: Total RNAs extracted from untransfected or stably transfected fibroblasts were subjected to RT-PCR analysis to reveal the relative abundance of hybrid and endogenous *ND1* and *ND4* mRNAs as well as *ATP6* mRNAs. 300 ng of each RNA preparation was electrophoresed on a formaldehyde-agarose gel to assess the integrity of RNA preparations (upper-left panel). The amount of RNAs required for the reverse transcription, PCR conditions and specific oligonucleotides used for each gene are summarized in Table 1. Signals obtained from the endogenous *ND1* gene are shown in lines 1, 4, 7 and 10. The endogenous *ND4* mRNA results are presented in lines 3, 6, 9 and 12. Hybrid mRNA signals are shown in lines 2 and 6 for *ND4*; 8 and 11 for *ND1*. Hybrid mRNAs were never detected neither in untransfected cell RNAs (lines 2 and 8) nor in control RNAs (unpublished data). Steady-state levels of the endogenous *ND1*, *ND4* and *ATP6* mRNAs were comparable in all the RNA preparations. The amounts of *ND1* and *ND4* hybrid mRNAs were similar in LHON #2 + *WT-ND1* and LHON #1 + *WT-ND4*. However, hybrid mRNAs were less abundant than their endogenous counterparts since 6 times more RNA and additional 10 cycles of PCR were required to detect similar signals of the amplified products (Table 1; lines 5 and 6; lines 11 and 12). B: Two independent protein extracts were obtained from digitonin-permeabilized fibroblasts from a control subject, LHON #1, LHON #2 patients and their counterparts allotopically expressing the wild-type *ND4* and *ND1* genes and subjected to Western blot analysis. Immunoblotting analysis was performed using anti-ATP synthase α-subunit (ATPα), anti-Flag M2 (FLAG) and anti-ND1 antibodies (ND1) (left panel). As implied by the molecular weight markers (Bench Mark Pre-stained Protein ladder, Invitrogen), the apparent molecular weight of each protein band was not too different from their theoretical molecular weights (http://www.mitomap.org/): *ND1* ~33 kDa, *ND4* ~53 kDa. A weaker band was always detected with both anti-Flag and anti-ND1 antibodies in LHON #2 + *WT-ND1* cells of about ~37 kDa that could correspond to the precursor form of the fusion protein (*). The ATPα protein had an apparent molecular weight of ~65 kDa as previously observed in HeLa cells [34]. Densitometric analyses were performed with signals obtained for three independent Western blots in which each protein extract was tested (Quantity One Biorad software system). Bar graphs in the right panel compared the overall ND1 signal after normalization with the ATPα signal. A significant decrease on the relative amount of the ND1 protein was observed in fibroblasts from LHON #2 when compared with either control or LHON #1 fibroblasts, according to the paired Student's *t*-test ($p=0.0078$ and 0.003; $n=6$). In LHON #2 fibroblasts allotopically expressing the wild-type *ND1* gene, the ND1 antibody recognized both the endogenous and the fusion ND1 proteins since the intensity of the protein-signal increased of approximate 1.8-fold. Further, intensities of the two signals were significantly different according to the paired Student's *t*-test ($p=0.0016$; $n=6$).

2.6. Protein extract and Western blot analysis

Protein extraction was essentially performed according to Nijtmans et al. [35]. Briefly, one 75-cm^2 flask of fibroblasts was trypsinized (about 2–4 millions of cells depending of the confluence) and washed twice with cold phosphate-buffered saline (PBS). Cells were incubated 10 min on ice with cold digitonin (8 mg/ml in PBS, v/v) to dissolve membranes. Digitonin was diluted by addition of cold PBS. Cells were spun for 5 min, at 10,000 ×*g* at 4 °C. The pellet was washed once more in 1 ml cold PBS. To solubilize, the pellet was vigorously pipetted in buffer A containing 1.5 M aminocaproic acid and 50 mM Bis–Tris/HCl, pH 7.0. Next, cells were incubated at 0 °C for 5 min by addition of dodecylmaltoside (10% w/v). Cells were centrifuged at 20,000 ×*g* for 30 min at 4 °C. Pellet was resuspended in buffer A. The protein concentration was estimated by the Bradford protein assay (Sigma), with BSA as standard. After denaturation at 70 °C, 8 μg proteins were separated by SDS-PAGE, using a 4–12% polyacrylamide gel (NuPAGE® system, Invitrogen) and transferred to a nitrocellulose membrane (GE Heathcare). Membranes were probed with mouse monoclonal antibodies anti-Flag M2 (3.5 μg/mL) or anti-ATP synthase α-subunit (0.5 mg/mL) and with a polyclonal anti-ND1 subunit antibody kindly provided by Dr. A. Lombes (1:800). Immunoreactive bands were visualized with an anti-mouse or anti-rabbit antibodies coupled to horseradish peroxidase (0.1 μg/mL) followed by ECL Plus detection (GE Heathcare).

2.7. Biochemical assays

Rotenone-sensitive complex I, oligomycin-sensitive complex V activities and ATP synthesis rate were assayed as recently described [32,36]. Antimycin-sensitive quinol cytochrome *c* reductase (complex III activity) was measured as previously described [37]. The quinone derivative used to measure complex III was decylubiquinol [37]. Complex IV activity is triggered by the addition of reduced cytochrome *c* [36]. Note that when half the cytochrome *c* has been oxidized, the rate of cytochrome *c* oxidation is reduced by about half. Measurement of the three respiratory chain complexes was achieved from a single culture of skin fibroblasts from patients and the control subject and repeated for at least 12 times. Stably transfected fibroblasts have been monitored several times (4–12) using two independent stably transfected cells per patient. Each assay was performed with 2×10^5 cells. Protein concentration was measured with the Bradford assay. All chemicals were of the highest grade from Sigma (St. Louis, MO).

2.8. Statistics

Differences between control fibroblasts, untransfected and transfected LHON fibroblasts were assessed using the paired Student's *t*-test with a minimal significance of $p<0.05$.

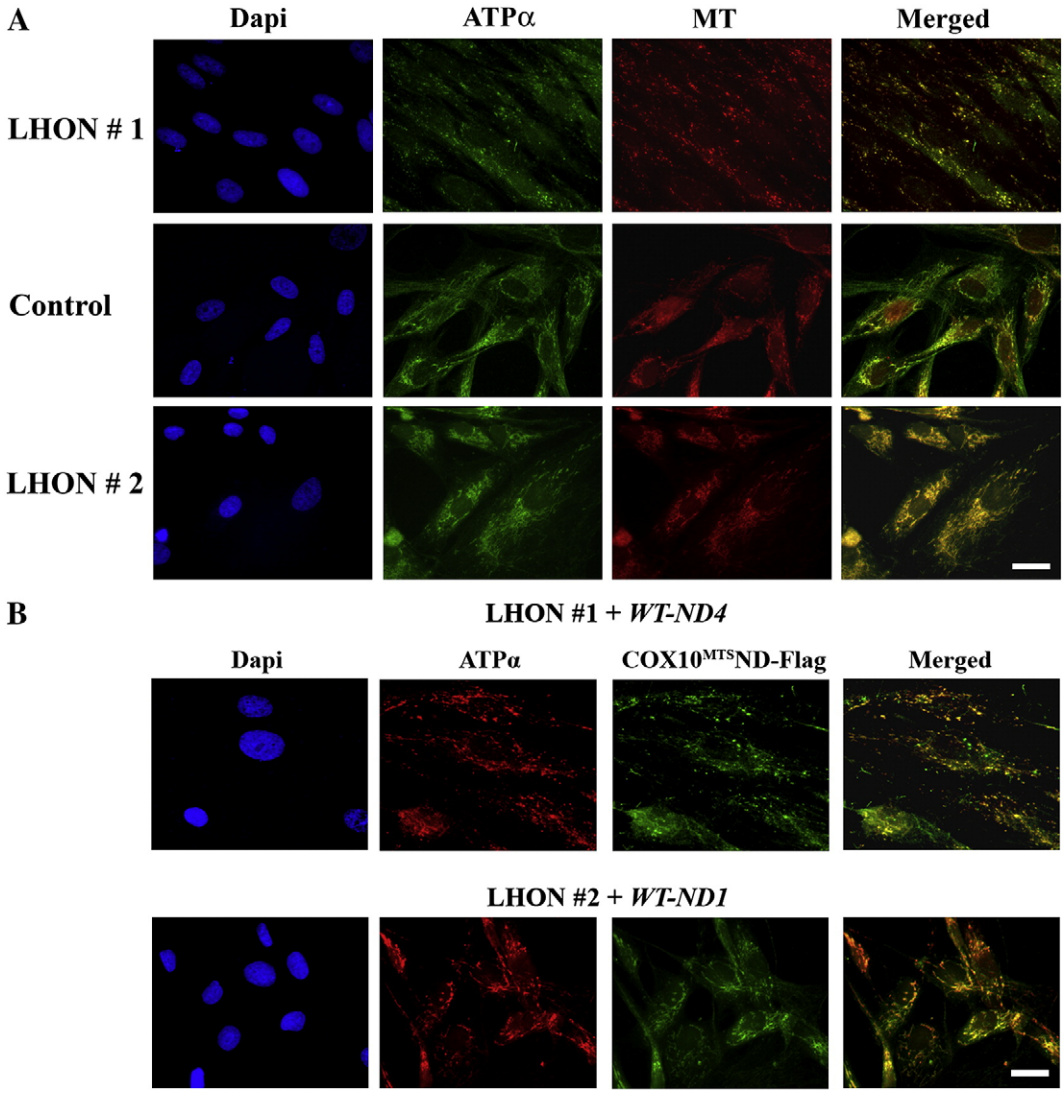

Fig. 2. Mitochondrial morphology in control fibroblasts, untransfected and transfected LHON fibroblasts. A: Mitochondrial shape in fibroblasts from two LHON patients and from a healthy control subject were examined by indirect immunofluorescence using antibody against the ATP synthase α-subunit (ATPα). The membrane potential-dependent probe MitoTracker Red CMXRos (MT) was used as a specific mitochondrial marker. The merged panel showed a significant colocalization between ATP synthase α signal and MT staining. The bar corresponds to 15 μm. B: Subcellular localization of the allotopically expressed proteins and the endogenous ATP synthase α-subunit protein *ex vivo*. Stably transfected LHON cells with *COX10*^{MTS}*ND4-3′UTR*^{COX10} (LHON #1+*WT ND4*) or *COX10*^{MTS}*ND1-3′UTR*^{COX10} (LHON #2+*WT-ND1*) plasmids were visualized by indirect immunofluorescence using antibodies against the Flag epitope (COX10^{MTS}ND-Flag) or against the ATP synthase α-subunit. A merged image of immunofluorescence revealed with each antibody is shown in the right panel. A significant colocalization of both COX10-ND1Flag, COX10-ND4Flag, and ATP synthase α signals was observed in the cells examined. Fluorescence was inspected with a Leica DM 5000 B Digital microscope. The bar corresponds to 15 μm.

3. Results

3.1. Steady-state levels of endogenous and hybrid mRNAs from the ND4 and ND1 genes, and of the fusion ND4 and ND1 proteins in stably transfected LHON fibroblasts

To estimate the efficiency of our constructions on directing the expression of nuclearly-encoded *ND4* and *ND1* genes, we analyzed in transfected cells the amount of hybrid mRNAs and compared it to endogenous *ND4* and *ND1* mRNAs by RT-PCR (Fig. 1A). The integrity of each RNA preparation was assessed by electrophoresis; no difference in 28S and 18S ribosomal RNA bands from the different RNA samples examined was observed confirming the integrity of the preparations (Fig. 1A upper-left panel). Moreover, the amount of the endogenous mitochondrial *ATP6* mRNA was similar in transfected and untransfected LHON fibroblasts (Fig. 1A, upper-right panel). Hybrid mRNAs produced from both *COX10*^{MTS}*ND4-3′UTR*^{COX10} and *COX10*^{MTS}*ND1-3′UTR*^{COX10} vectors were only detected in LHON #1+*WT ND4* and LHON #2+*WT ND1* fibroblasts respectively (Fig. 1A, bottom panel). Despite the strength of the CMV promoter, these cells did not accumulate very high levels of hybrid *ND4* and *ND1* mRNAs as compared to endogenous mRNAs. Indeed as shown in Table 1, 35 cycles of amplification and 300 ng of RNA extraction were required to obtain an amount of PCR product for hybrid mRNAs comparable to the one detected from the endogenous mRNAs, which only needed 50 ng of RNAs and 25 cycles of amplification.

To determine whether hybrid mRNAs were translated in detectable levels of fusion wild-type ND4 and ND1 proteins, protein extracts from digitonin-permeabilized fibroblasts were subjected to Western-blotting analyses. Immunoblots were first performed using anti-ATP synthase α antibody. This naturally imported mitochondrial protein of respiratory complex V was present, as a single band of approximately 65 kDa, in similar amount in all cells tested (Fig. 1B). The anti-Flag antibody was used to detect the fusion proteins, since a flag epitope was appended in frame to the C-terminus of each protein. The antibody revealed one band of approximate 53 kDa in fibroblasts transfected with the *COX10*^{MTS}*ND4-3′UTR*^{COX10} vector (LHON #1+*WT-ND4*), and two forms of about 37 (*) and 33 kDa in cells expressing the *COX10*^{MTS}*ND1-3′UTR*^{COX10} gene (LHON #2+*WT-ND1*), as implied by the molecular weight markers. The larger band could represent the precursor form of the fusion ND1 protein; indeed its signal was always weaker as compared to the one detected for the form of about 33 kDa. Both ND4 and ND1 fusion proteins detected by the anti-Flag antibody presented electrophoretical properties similar to the ones expected from their theoretical molecular weights of approximate 51.69 kDa and 35.66 kDa respectively (http://www.mitomap.org/). No signal was detected with the anti-Flag antibody in the other samples examined. The amount of ND1 protein was compared in each protein extract using a polyclonal anti-ND1 subunit antibody (Fig. 1B). Noticeably, the amount of the endogenous ND1 protein was low in fibroblasts bearing the 3460/*ND1* mutation. After normalization with the amount of ATP synthase α, a 2.7 or 2.1-fold reduction in the amount of ND1 protein in these cells was observed when compared to control fibroblasts and fibroblasts harboring the 11778/*ND4* mutation respectively. In fibroblasts expressing the *COX10*^{MTS}*ND1-3′UTR*^{COX10} gene (LHON #2+*WT-ND1*), the anti-ND1 antibody was able to recognize both the endogenous and the fusion protein. Indeed the difference between these fibroblasts and controls or fibroblasts harboring the 11778/*ND4* mutation was of only 1.46 and 1.3-fold respectively (Fig. 1B, right panel). Additionally, the anti-ND1 antibody detected a slightly larger

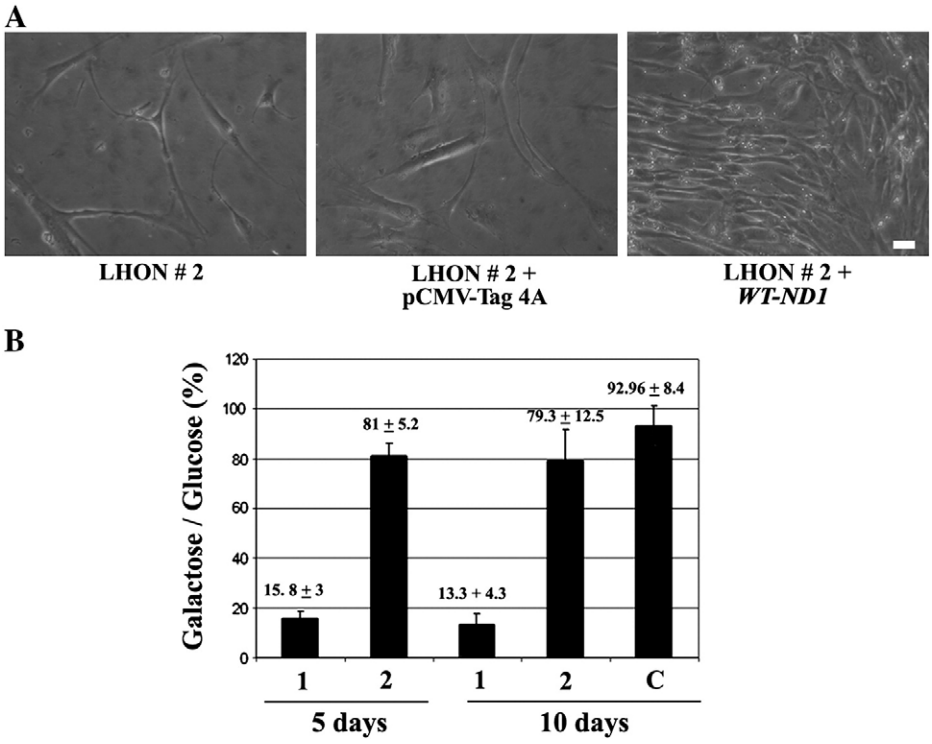

Fig. 3. A fibroblast' ability to grow in galactose selective medium. A: After 10 days of growth in galactose medium, LHON #2 untransfected fibroblasts and LHON #2 fibroblasts transfected with either the *pCMV-Tag 4A* vector or with the *COX10*^{MTS}*ND1-3′UTR*^{COX10} plasmid (LHON #2+*WT-ND1*) were observed by photonic microscope (10×, the bar represent 20 μm). Cells allotopically expressing the wild-type version of *ND1* exhibited a substantial increase in growth rate in galactose medium compared to untransfected and mock-transfected LHON #2 fibroblasts. B: Cell survival after 5 or 10 days of galactose selection measured in LHON #2 cells transfected with the *pCMV-Tag 4A* vector (1) and LHON #2 fibroblasts transfected with the *COX10*^{MTS}*ND1-3′UTR*^{COX10} plasmid (2). The two transfected fibroblasts were compared to control fibroblasts (C) after 10 days of galactose selection. Bar graphs represented the cell growth capacity in galactose compared to that in glucose. One hundred percent represents the total number of cells that grew in glucose medium for each tested cells. Experiments were performed six times, Student's *t*-test established that the abilities to grow in galactose were significantly improved in the transfected cells (*COX10*^{MTS}*ND1-3′UTR*^{COX10}) compared to mock-transfected cells ($p<0.0001$, $n=6$).

Table 2
Ability of LHON fibroblasts carrying the *ND1* mutation and their counterparts expressing the recoded *ND1* gene to grow in galactose medium

	Number of cells/ml (glucose)	Number of cells/ml (galactose)	Survival rate % (galactose/glucose)
LHON #2+ *pCMV-Tag 4A*	31250±957	4300±600	13,76
Control	31075±4728	28500±4102	91.7
LHON #2+ *WT-ND1*	34325±4261	23950±3879	69.8

The viability of stably transfected cells with either the *pCMV-Tag 4A* vector (LHON #2+*pCMV-Tag 4A*) or the *COX10*^{MTS}*ND1-3′UTR*^{COX10} vector (LHON #2+*WT-ND1*) was measured after 14 days of growth in either glucose- or galactose-containing media and compared to control fibroblasts. Four independent experiments were performed and the amount of viable cells under each condition was obtained by counting with Malassez plates. The overall number of viable cells in galactose medium was significantly different according to the Student's *t*-test when LHON #2+*WT-ND1* and LHON #2+*pCMV-Tag 4* fibroblasts were compared ($p=0.0016$, $n=4$) as well as for LHON #2+*pCMV-Tag 4 versus* control fibroblasts ($p=0.0014$, $n=4$). In contrast, no significant difference was evidenced in the total number of cells after 14 days of growth in galactose between LHON #2+*WT-ND1* and control fibroblasts ($p=0.28$, $n=4$).

band in transfected fibroblasts, as the anti-Flag antibody did, which could correspond to the precursor form of the fusion ND1 protein (Fig. 1B, bottom panel *). These results indicate that optimized allotopic expression led to the production of detectable amounts of the fusion ND4 and ND1 proteins. Interestingly in LHON #2 fibroblasts, we observed that both the endogenous *ND1* gene and the one synthesized from our vector directed the synthesis of similar amounts of proteins. The question arises whether the fusion ND4 and ND1 proteins localize to mitochondria and can compensate the defective endogenous protein in these cells.

3.2. Mitochondrial subcellular distribution of allotopic ND1 and ND4 gene products in human fibroblasts

First, we examined the mitochondrial morphology in fibroblasts from two patients harboring the G11778A *ND4* (LHON #1) and G3460A *ND1* (LHON #2) substitutions. We used the membrane potential-dependent probe MitoTracker Red CMXRos as a mitochondrial marker as well as a monoclonal antibody directed against the α-subunit of mitochondrial ATP synthase. The two labelings are perfectly superimposable (see Fig. 2A, merged panel). In about 90% of LHON #1 fibroblasts, both the anti-ATP synthase α-subunit monoclonal antibody and the MitoTracker probe revealed a punctuate distribution of fluorescent dots, as recently described [32] (Fig. 2A). This mitochondrial fragmented appearance may indicate a perturbation in the balance between the organelle fusion and fission in these cells. The remaining cells showed long and tiny filaments around the nuclear envelop. By contrast, in 90% of LHON #2 fibroblasts, mitochondria appeared more elongated and with a shape more complex than in LHON #1 fibroblasts (Fig. 2A). The mitochondrial morphology in the two patient fibroblasts was undeniably different. Additionally, in fibroblasts from a healthy subject (Fig. 2A, Control) less than 5% cells showed a fragmented mitochondrial morphology. Thus, control fibroblasts and fibroblasts from the LHON #2 patient displayed a similar mitochondrial morphology. This observation suggests that in fibroblasts examined the *ND4* mutation reduced mitochondrial shape complexity at a higher extent than the *ND1* mutation.

Fibroblasts from the two patients were subsequently stably transfected with constructions leading to the expression of engineered nucleus-localized wild-type *ND4* or *ND1* genes, respectively. To increase the probability for the hydrophobic ND1 or ND4 precursors to be efficiently translocated inside mitochondria, we combined to the *ND4* and *ND1* ORFs the sequence encoding the MTS and the 3′UTR from the *COX10* gene, as we recently reported [32]. Then, we examined by indirect immunofluorescence the ability of the proteins synthesized from these plasmids to localize to mitochondria using the anti-Flag antibody. There was a colocalization of the anti-Flag and the ATP synthase α-subunit antibodies for each transfected fibroblasts examined (Fig. 2B). The overlay of the two specific antibody labelings indicates that allotopically expressed proteins and the endogenous mitochondrial ATP synthase α-protein were distributed in the same subcellular compartment *in vivo*. Moreover, in fibroblasts allotopically expressing the *COX10*^{MTS}*ND4-3′UTR*^{COX10} vector (Fig. 2B, LHON #1+*WT-ND4*) we consistently observed a less dotted appearance of their mitochondria as compared to untransfected fibroblasts (Fig. 2A) or fibroblasts transfected with the *pCMV-Tag 4A* vector (unpublished data). Mitochondria appeared more elongated and networks were visualized in approximately 40% of cells, indicating that the mitochondrial shape in LHON #1 after transfection became more comparable to the one observed in both control and LHON #2 fibroblasts. Thus, the optimized allotopic expression of the wild-type *ND4* and *ND1* genes in fibroblasts carrying these genes mutated led to the accumulation of fusion proteins in the mitochondrial compartment.

3.3. The ability to grow in galactose medium is improved in LHON fibroblasts carrying the G3460A substitution by the allotopic expression of ND1 gene

It has been well documented that when galactose replaces glucose as the carbon source in the medium, cells deficient in mitochondrial function are greatly curtailed in their growth rate [15,38]. We have recently described a 3.5-fold decrease in the growth rate of LHON #1 fibroblasts compared to control cells after 8 days of growth in galactose medium. This decrease was compensated when LHON #1 fibroblasts allotopically expressed the *COX10*^{MTS}*ND4-3′UTR*^{COX10} vector [32]. To determine whether LHON #2 fibroblasts presented also a curtailed growth rate in galactose and to evaluate the impact of *ND1* allotopic expression, the overall number of cells transfected with either the *pCMV-Tag 4A* or the *COX10*^{MTS}*ND1-3′UTR*^{COX10} vectors was estimated after 5 or 10 days of culture in either glucose or galactose media; immediately after transfection. Fig. 3A shows a striking negative impact on cell survival after 10 days of culture in galactose medium in untransfected LHON #2 cells and their counterparts transfected with the *pCMV-Tag 4A* plasmid as compared to fibroblasts allotopically expressing the wild-type gene. Fibroblasts from a healthy subject did not show differences in their growth rates when glucose- or galactose-containing medium were measured. Indeed, after 10 days of growth in galactose the overall amount of cells was 92.96%±8.4 compared to the cells grown in glucose (Fig. 3A; $p=0.20$, $n=6$). We observed an approximately 7-fold decrease in the growth rate of LHON #2 fibroblasts transfected with the *pCMV-Tag 4A* compared to control cells after 10 days of growth in galactose medium (Fig. 3B). LHON #2 fibroblasts expressing the *COX10*^{MTS}*ND1-3′UTR*^{COX10} vector (LHON #2+*WT-ND1*) showed a 5.1- and a 5.9-fold improvement ($p<0.0001$, $n=6$) after 5 and 10 days in their ability to grow in galactose compared to

Table 3
Measurement of mitochondrial ATP synthesis in digitonin-permeabilized fibroblasts

	μM ATP/min/10^6 cells/mg protein
	Pyruvate/malate
Control	2423.1±125.7
LHON #2	605.5±72.8
LHON+*pCMV-tag 4A*	730.4±76.5
LHON+*WT-ND1*	1979.0±168.8

The rate of ATP synthesis, expressed in μM ATP/min/10^6 cells/mg protein, was measured after 5 days of growth in glucose medium, in control fibroblasts, LHON #2 fibroblasts, LHON #2 fibroblasts stably transfected with the *pCMV-tag 4A* vector and LHON #2 fibroblasts stably transfected with *COX10*^{MTS}*ND1-3′UTR*^{COX10} plasmid (LHON #2+*WT-ND1*). Three independent experiments were performed using pyruvate/malate (complex I-linked substrates). No significant difference in the ATP synthesis capacity was observed between control cells and fibroblasts allotopically expressing *ND1* for complex I-linked substrates, confirming the rescue of the respiratory chain defect.
ATP, adenosine triphosphate; LHON, Leber's Hereditary Optic Neuropathy.

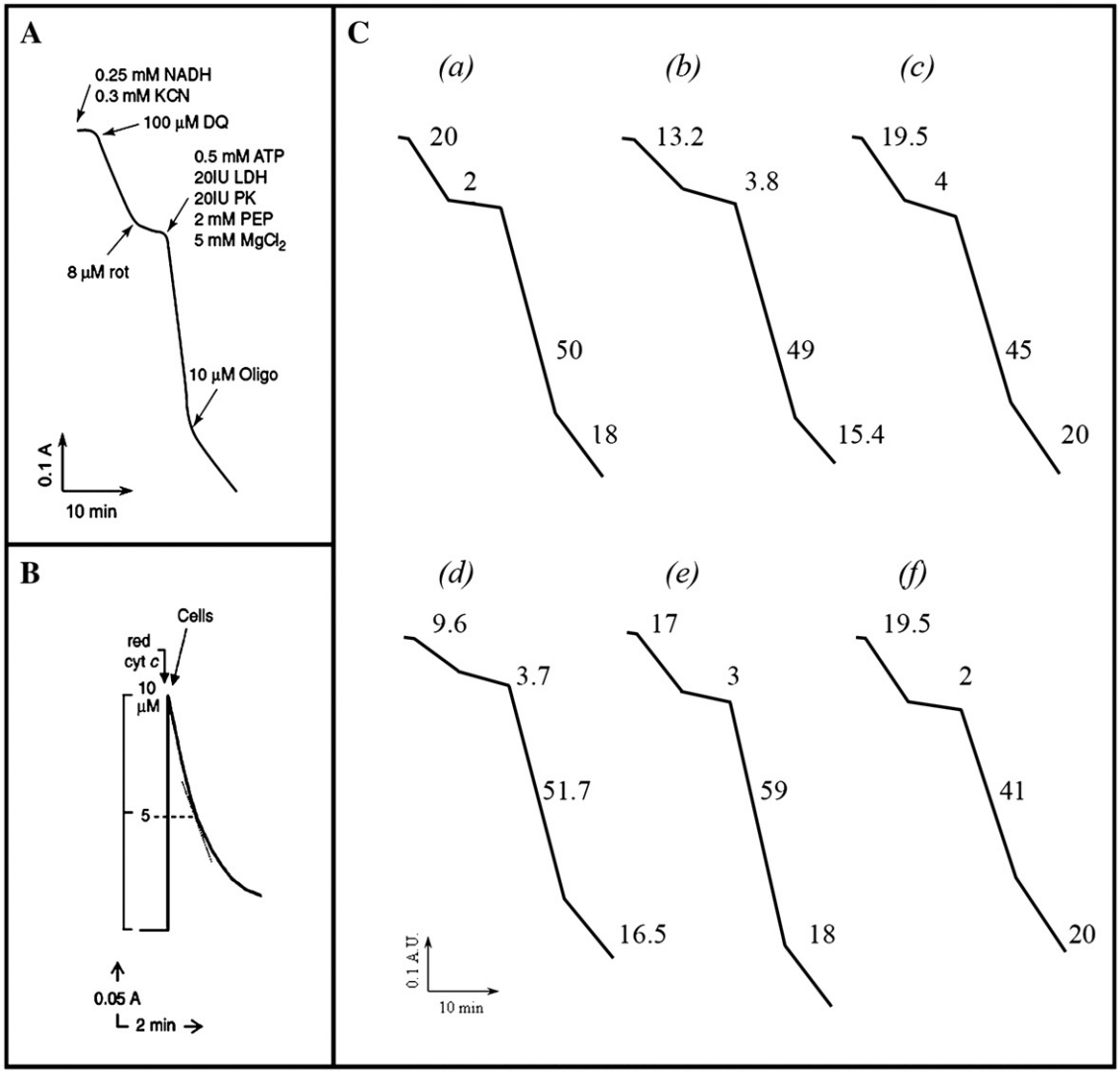

D

	IV / I	V / I	III/IV
Control	28.96 ± 4.24 (n = 12)	1.35 ± 0.50 (n = 9)	2.10 ± 0.43 (n = 5)
LHON #1	49.16 ± 11.70 (n = 12)	3.22 ± 0.37 (n = 9)	1.80 ± 0.42 (n = 5)
LHON #1 + *WT-ND4*	25.71 ± 5.66 (n = 12)	1.66 ± 0.49 (n = 9)	ND
LHON #2	75.4 ± 21.86 (n = 5)	5.52 ± 0.75 (n = 5)	1.98 ± 0.53 (n = 5)
LHON #2 + *WT-ND1*	55.86 ± 6.76 (n = 3)	2.30 ± 0.67 (n = 3)	ND
NARP + *WT-ATP6*	18.35 ± 2.16 (n = 8)	1.16 ± 0.16 (n = 8)	ND

Fig. 4. Restoration of complex I activity in LHON-transfected fibroblasts. A: Illustrative curve for the successive measurement of rotenone-sensitive complex I and oligomycin-sensitive complex V activities. B: Typical curve for the measurement of cytochrome *c* activity. C: Enzymatic activity measurement of rotenone-sensitive complex I and oligomycin-sensitive complex V activities for control fibroblasts (a), LHON #1 (b), LHON #1+*WT-ND4* (c), LHON #2 (d) LHON #2+*WT-ND1* (e) and NARP+*WT-ATP6* (f). ATP, adenosine triphosphate; cyt, cytochrome; DQ, duroquinone (oxidized); KCN, potassium cyanide; LDH, lactate dehydrogenase; MgCl2, magnesium chloride; NADH, reduced nicotinamide adenine dinucleotide; oligo, oligomycin; PEP, phosphoenol pyruvate; PK, pyruvate kinase; red, reduced. Numbers along the traces corresponds to activity expressed as nmol/min/mg protein. D: Table shows the enzyme activities ratio (IV/I), (V/I) and (III/IV) for control fibroblasts (Control), untransfected LHON cells (LHON #1 and LHON #2), LHON fibroblasts allotopically expressing *ND1* or *ND4* (LHON #1+*WT-ND4* and LHON #2+*WT-ND1*) and NARP cells allotopically expressing *ATP6* used as control (NARP+*WT-ATP6*). The number of experiments was indicated in brackets. The difference between LHON #1 and LHON #1+*WT-ND4* was statistically significant ($p<0.0001$, $n=12$ for IV/I; $p<0.0001$, $n=9$ for V/I). For LHON #2, the ratio of V/I activity was also significantly different when the couple LHON #2 and LHON #2+*WT-ND1* was compared ($p=0.0005$, $n=3$). No significant difference was observed between control and LHON fibroblasts in the enzyme activity ratio (III/IV): $p=0.45$ and 0.61, $n=5$ for LHON #1 and LHON #2 respectively).

LHON #2 fibroblasts transfected with the *pCMV-Tag 4A* plasmid (Fig. 3B).

To further evaluate the impact of *ND1* allotopic expression on the growth rate in galactose medium the number of stably transfected cells with either the *pCMV-Tag 4A* or the *COX10*^{MTS}*ND1-3′UTR*^{COX10} vectors were evaluated after 14 days of growth in either glucose or galactose media and compared to the overall number of viable cells for control fibroblasts under the same conditions (Table 2). The survival rate on galactose medium was improved of about 5.1 fold ($p=0.0016$, $n=4$) in cells expressing the recoded *ND1* gene, strengthening the data obtained immediately after transfection. Moreover, cell growth rates in galactose were not statistically different between control cells and fibroblasts allotopically expressing the *ND1* gene after 14 days of selection ($p=0.28$, $n=4$).

Thus, as we have recently reported for cells carrying the *ND4* G11778A substitution [32], the allotopic expression of the engineered nucleus-localized *ND1* gene led to a significant benefit for mitochondrial function measured by the ability to growth in galactose of cells harboring the G3460A substitution.

3.4. Decrease of ATP synthesis in LHON #2 fibroblasts was rescued by the allotopic expression of ND1

The impairment of energy metabolism due to mutations in mtDNA encoded genes has been frequently correlated with a reduced ability of cells harboring these mutations to synthesize ATP *in vitro* from ADP and Pi through the action of respiratory chain complex V [39]. Therefore, to further confirm that allotopically expressed *ND1* gene product was functional within complex I, oligomycin-sensitive ATP production by digitonin-permeabilized fibroblasts was measured using complex I-linked (malate/pyruvate) substrates (Table 3). For LHON #2 fibroblasts, we evidenced a 75% reduction in the rate of complex I-dependent ATP synthesis when compared to controls ($p=0.0004$, $n=3$). When LHON #2 fibroblasts were transfected with the mock vector, we showed a decrease of approximatively 70% in ATP synthesis statistically significant for complex I-linked substrates ($p<0.0001$, $n=3$ for pyruvate/malate). ATP synthesis measurement in LHON fibroblasts allotopically expressing the engineered *ND1* gene (LHON #2+*WT-ND1*) indicated an almost complete recovery in the rate of complex I-dependent ATP production (80% relative to control). A statistically significant difference was reached between LHON #2 fibroblasts and cells allotopically expressing the *ND1* gene: $p=0.0018$, $n=3$ for pyruvate/malate (Table 3). The difference between cells expressing *ND1* and mock-transfected fibroblasts was also significant ($p=0.003$, $n=3$ for pyruvate/malate). These data establish that the allotopic expression of *ND1* corrected the energy metabolism impairment of fibroblasts harboring the G3460A *ND1* substitution.

3.5. The allotopic expression of ND4 or ND1 genes leads to restoration of complex I activity in LHON fibroblasts harboring these genes mutated

Since, both *in vivo* and *in vitro* biochemical studies in different patient-derived tissues and cellular experimental models have produced conflicting results regarding the extent of respiratory chain dysfunction in LHON [8,9], we decided to perform spectrophotometric assays [36] to measure the activity of respiratory complexes I, III, IV and V in LHON fibroblasts and their counterparts stably transfected with either *ND4* or *ND1* genes. In these experiments, we also used NARP fibroblasts allotopically expressing *ATP6* gene as an internal control of fully respiratory chain function recovery [32] (Fig. 4). These measurements allow to estimate the severity of respiratory chain defects in these fibroblasts and to further validate the rescue by the optimized allotopic expression approach. We consistently observed differences in the rotenone-sensitive complex I activity (I) between control fibroblasts and LHON fibroblasts (Fig. 4C, compare a, b and d). By contrast, we did not observe significant differences between control, LHON #2+*WT-ND1*, LHON #1+*WT-ND4* and NARP+*WT-ATP6* kinetics (Fig. 4C, compare a, c, e and f). No significant difference was observed in the III/IV ratio between control, LHON #1 and LHON #2 fibroblasts (Fig. 4D). When the two enzymatic activity ratios (IV/I) and (V/I) were assessed, we noticed an increase in the two ratios in LHON fibroblast cells, indicating that they presented a marked defect in complex I activity. Indeed, we observed a 1.7- and 2.4-fold increase ($p<0.0001$) of LHON #1 fibroblasts and a 2.6- and 4-fold of LHON #2 fibroblasts in the IV/I and V/I ratios, respectively (Fig. 4D). Interestingly, fibroblasts allotopically expressing *ND4* and control fibroblasts revealed almost identical IV/I and V/I activity ratios. A statistical difference was reached between LHON #1 untransfected fibroblasts and their counterparts allotopically expressing the *ND4* gene ($p<0.0001$, $n=12$ for the IV/I ratio and $p<0.0001$, $n=12$ for the V/I ratio) (Fig. 4D). In LHON fibroblasts expressing the engineered *ND1* gene, we obtained a partial restoration of the complex I activity (60% for the V/I ratio). The difference between LHON #2 fibroblasts and cells expressing *ND1* was significant for this ratio ($p=0.0005$, $n=3$). Hence, the spectrometrically performed assay of complex I enzymatic activity in LHON fibroblasts harboring either the *ND4* or the *ND1* mutations was effective in the detection of a severe defect on these cells as compared to controls. Moreover, the measurements of complex III, IV and V activities clearly demonstrated that OXPHOS defect in these fibroblasts is restricted to complex I. Since a significant improvement of its activity was consistently noticed in stably transfected cells, the fusion ND4 and ND1 proteins synthesized from our vectors appear to be functional within the respiratory chain complex I and able to compensate for the endogenous defective gene products.

4. Discussion

Mitochondrial disorders can not be ignored anymore in most medical areas. They include specific and widespread organ involvement, with tissue degeneration or tumor formation. Primary or secondary actors, mitochondrial dysfunctions are also playing a role in the ageing process [40,41]. Research dealing with mitochondrial physiology and pathology has almost 20 years of history all over the world. Despite the progresses made in the identification of disease molecular bases, nearly all remains to be done regarding therapy [25]. The Leber's Hereditary Optic Neuropathy (LHON), a mitochondrial genetic disease, represents the main cause of male adolescent blindness. Its prevalence has been estimated at ~1 over 25,000 in the north east of England. Few data exist on the absolute prevalence of LHON for other populations, except in Australia where 2% of people on the blind register suffer from LHON [42]. Unfortunately since pathogenic mechanisms of LHON are not yet understood there are no efficient therapies for its treatment. Quantifications of complex I activity were controversial in cybrids which were used as cellular models to evaluate mitochondrial complex I defects in patients harboring LHON mutations [15,19]. Cybrid cells are valuable in mitochondrial research to better understand mechanisms of several pathologies with mitochondrial implications, but they remain an "artificial" system contrary to fibroblasts which are supposed to reproduce more accurately natural physiological responses. Additionally studies performed with muscle tissues or lymphocytes led also to contentious results. For example, Majander et al. did not observe any decrease in complex I activity in lymphoblasts harboring the *ND4* mutation [11] whereas Larsson et al. observed a 50% reduction [10]. Nonetheless, it has been well established that LHON patients with the *ND1* mutation are more affected than patients with the *ND4* mutation. Compilation of experimental data showed a 60 to 80% decrease in complex I activity in cells harboring the *ND1* mutation whereas only a 0 to 50% reduction was detected in cells bearing the *ND4* mutation [42]. Up until today, we were able to find only one report on LHON fibroblasts OXPHOS studies *ex vivo*. Cock et al. have reported an approximate 60% defect in mitochondrial NADH CoQ1 reductase

activity in cultured fibroblasts bearing the G3460A *ND1* mutation. However, complex I-linked ATP synthesis rate was normal in these fibroblasts [13]. We reported here using spectrophotometric measurements that skin fibroblasts carrying the *ND1* (LHON #2) and *ND4* (LHON #1) mutations presented consistent 80% and 60% decreases in complex I activity respectively. This is probably due to the high sensitivity and robustness of the spectrometric assay performed [36]. Indeed, the sequential determination of complex activities on the same sample allows the determination of enzyme activity ratios. This latter parameter has been previously shown to be the most efficient for detecting isolated and partial impairment of respiratory chain activity [43].

Notably, the cellular morphology of mitochondria in LHON #1 fibroblasts always showed punctuate dots suggesting an enhanced organelle fission in these cells in contrast to the LHON #2 fibroblasts or control fibroblasts which revealed more elongated and more branched mitochondria. Recently, Koopman et al. evidenced a relationship between complex I deficiency in fibroblasts obtained from patients carrying mutations in nuclear genes encoding complex I subunits and the mitochondrial shape. These authors claimed that changes in mitochondrial morphology ("mitochondrial complexity") are directly dependent on the severity of complex I deficiency. They distinguished two categories of fibroblasts: one presenting fragmented mitochondria, severe complex I amount and activity defects. The second group displayed a normal mitochondrial appearance and moderate complex I defects [44]. From our observations, LHON #1 fibroblasts would be categorized in the "fragmented mitochondria" group while LHON #2 cells would belong to the "normal appearance" group. However, the morphology difference does not correlate with the severity of complex I deficiency extent, since LHON #2 cells with normal mitochondrial appearance presented the more severe complex I defect. Alternative explanations should therefore be envisaged. For example, differential effects on morphology might be associated with differences in the role of *ND1* and *ND4* in complex I assembly, and thus in mitochondrial organization [45,46]. There is also a possibility that "mitochondrial complexity" could be more dependent on nuclear genes encoding mitochondrial proteins as described for the *OPA1* gene product involved in Dominant Optic Atrophy [7]. Interestingly, upon allotopic expression of *ND4* gene LHON #1 fibroblasts, the overall mitochondrial morphology became similar to the "normal" class and to both control and LHON #2 fibroblasts (Fig. 2B).

In a previous study, we measured two independent parameters of mitochondrial function in LHON fibroblasts harboring the *ND4* mutation (LHON #1) and their counterparts allotopically expressing the wild-type gene: (i) cells' ability to grow in a galactose-containing medium that relies on oxidative phosphorylation and (ii) cells' capacity to produce ATP *in vitro*. According to these two criteria, we have demonstrated that optimized allotopic expression of the wild-type *ND4* gene allowed a long-lasting benefit for mitochondrial function in these cultured fibroblasts harboring the *ND4* mutation [32]. In the present study, we established unequivocally the complete restoration of OXPHOS function in these fibroblasts by measuring complex I, IV and V activities. Indeed, by analyzing two independent stably transfected fibroblasts with the $COX10^{MTS}ND4\text{-}3'UTR^{COX10}$ vector, no significant difference was detected between these transfected cells and controls regarding complex I enzymatic activity. The increased number of experiments, compared to our previous work [32] allowed to statistically confirm the restoration of complex I activity in stably transfected cells (V/I ratios of 1.66±0.49 and 1.35±0.50 in patient cells and controls respectively, Fig. 4). Subsequently, our goal was to alleviate mitochondrial dysfunction in fibroblasts carrying the G3460A mutation (LHON #2) using *ND1* optimized allotopic expression. These engineered fibroblasts retained a long-term expression of the *ND1* gene and were able to survive for up to 14 days in a medium in which glucose had been replaced by galactose. To further validate that our approach conferred a real improvement of mitochondrial function in LHON #2 fibroblasts we measured the actual mitochondrial ATP synthesis capacity of cells allotopically expressing the wild-type gene. Stably transfected cells displayed a significantly improved ATP synthesis rate when complex I substrates were used. The overall ATP production rate of these cells became 80% relative to controls (Table 3). Since we were aware that increased ATP synthesis cannot be viewed as unequivocal evidence of rescue of mitochondrial dysfunction we spectrometrically assessed complex I enzymatic activity in untransfected and transfected LHON #2 fibroblasts as we did for LHON #1 cells. For LHON #2 fibroblasts, our optimized allotopic approach led to a partial but significant rescue of complex I defect. The amount determination of the ND1 protein presenting the deleterious substitution of an alanine by a threonine at codon 52 (A52T) in patient's fibroblasts showed that there was a clear diminution of about 2.7-fold when compared to normal fibroblasts. This striking diminution can explain why the inactivation of complex I is more pronounced in LHON #2 (*ND1*/3460) than in LHON #1 (*ND4*/11778) fibroblasts (80% vs. 60%). Moreover, it is considered that *ND1* plays a central role in the first step of complex I biogenesis. *ND1* is found in a separate, smaller complex before its association with other ND subunits [45,46]. Since LHON #2 fibroblasts accumulated significant lesser amount of *ND1* than control cells, this might be more detrimental to the functional assembling of complex I than the *ND4* mutation. When LHON #2 fibroblasts allotopically expressed the wild-type gene, an unambiguous 1.85-fold increase in the overall amount of ND1 proteins was evidenced resulting in a partial but significant restoration of complex I activity. Thus, we believe that the protein synthesized from our vector is directly responsible of complex I activity restoration. Two mechanisms can be envisaged: (1) the A52T substitution is detrimental for the endogenous protein that could become instable and unable to be recruited in the multimeric complex I. In this case the fusion protein can take its place during its biogenesis (2) conversely, even instable at least some ND1 molecules could be incorporated in complex I and in cells expressing our vector, the fusion protein, expressed at comparable levels, is able to replace the defective one within the complex and thus rescuing partially the complex I defect.

Finally, we have measured the IV/I and III/IV complex activity ratios in both LHON fibroblasts to determine whether complex I defect in these cells is associated to either complex IV or complex III decreased activities. Both complex activities were similar in these cells to that of controls and confirmed that they presented an isolated complex I deficiency which was significantly alleviated by using the optimized allotopic expression approach. Hence, our approach has led to the accumulation of sufficient amounts of functional proteins synthesized from our vectors (Fig. 1) which created a situation very similar to the heteroplasmy found in some patients suffering from mtDNA-related diseases (coexistence of both wild-type and mutated mtDNA molecules). The heteroplasmy achieved at the protein level by the optimized allotopic expression approach drives to the restoration of complex I activity and the improvement of the overall mitochondrial function in these cells.

4.1. Concluding remarks

In conclusion, we are as involved as many other laboratories worldwide in the challenge to find ways for fighting mitochondrial diseases. However, our main limitation is the absence of animal and cellular models required for both the understanding of the molecular mechanisms underlying the diseases and to evaluate therapeutic strategies, especially for mtDNA mutations. Last year, Qi et al. showed that the nuclear version of the mutant ND4 subunit of complex I is translocated into the mitochondria of mouse retinal ganglion cells and led to retinal and optic nerve degeneration. This important data represents a first step for the generation of a murine model resembling LHON [47]. Nevertheless, their approach encounters the

limitation of the inefficient mitochondrial import of the protein since the corresponding mRNA cannot be sorted to the mitochondrial surface. Hence, we suspect that it is not a robust mouse model to evaluate putative treatments. Besides, their strategy has the potential to become toxic for mouse retina over time, indeed high levels of misfolded hydrophobic proteins in the cytosol have been shown to be deleterious *ex vivo* [29].

The data presented here and our previous work definitely confirmed for three mitochondrial genes (*ATP6*, *ND4* and *ND1*) that the optimized allotopic approach based on the mRNA sorting to the mitochondrial surface is a suitable way for rescuing mitochondrial deficiencies caused by mutations in mtDNA genes. Our next challenge is to create an animal model resembling LHON and its cure using our optimized allotopic expression approach that will open the door to gene therapy for LHON (Ellouze et al., submitted).

Acknowledgements

We thank Drs. A. Munnich and J. Kaplan (INSERM U781, Paris) who kindly provided LHON fibroblasts and Dr. A. Lombes (INSERM U582, Paris) who provided the anti-ND1 antibody. We are also grateful to V. Forster for her assistance and advices on cell culture techniques. This work was supported by funds from the INSERM (U592), and Agence National pour la Recherche (ANR)/Maladies Rares. C. B. is the recipient of the Ouvrir les Yeux Association' awards and the ANR/Maladies Rares funding, S.E. is the recipient of an Ile de France fellowship, AB is supported by the INSERM and the ANR, and S. A. was supported by RETINA FRANCE and the Carnot Institute. P.B. and P.R. were supported by the Integrated European Project Eumitocombat and the Association Française contre les Myopathies.

References

[1] A.M. Schaefer, R. McFarland, E.L. Blakely, L. He, R.G. Whittaker, R.W. Taylor, P.F. Chinnery, D.M. Turnbull, Prevalence of mitochondrial DNA disease in adults, Ann. Neurol. 63 (2008) 35–39.
[2] M.Y. Yen, A.G. Wang, Y.H. Wei, Leber's hereditary optic neuropathy: a multifactorial disease, Prog. Retin. Eye Res. 25 (2006) 381–396.
[3] D.C. Wallace, G. Singh, M.T. Lott, J.A. Hodge, T.G. Schurr, A.M. Lezza, L.J. Elsas 2nd, E.K. Nikoskelainen, Mitochondrial DNA mutation associated with Leber's hereditary optic neuropathy, Science 242 (1988) 1427–1430.
[4] N. Howell, I. Kubacka, M. Xu, D.A. McCullough, Leber hereditary optic neuropathy: involvement of the mitochondrial *ND1* gene and evidence for an intragenic suppressor mutation, Am. J. Hum. Genet. 48 (1991) 935–942.
[5] D.R. Johns, M.J. Neufeld, R.D. Park, An ND-6 mitochondrial DNA mutation associated with Leber hereditary optic neuropathy, Biochem. Biophys. Res. Commun. 187 (1992) 1551–1557.
[6] C.Y. Yu Wai Man, P.F. Chinnery, P.G. Griffiths, Optic neuropathies—importance of spatial distribution of mitochondria as well as function, Med. Hypotheses 65 (2005) 1038–1042.
[7] V. Carelli, C. La Morgia, L. Iommarini, R. Carroccia, M. Mattiazzi, S. Sangiorgi, S. Farne, A. Maresca, B. Foscarini, L. Lanzi, M. Amadori, M. Bellan, M.L. Valentino, Mitochondrial optic neuropathies: how two genomes may kill the same cell type? Biosci. Rep. 27 (2007) 173–184.
[8] M.D. Brown, The enigmatic relationship between mitochondrial dysfunction and Leber's hereditary optic neuropathy, J. Neurol. Sci. 165 (1999) 1–5.
[9] N. Howell, LHON and other optic nerve atrophies: the mitochondrial connection, Dev. Ophthalmol, 37 (2003) 94–108.
[10] N.G. Larsson, O. Andersen, E. Holme, A. Oldfors, J. Wahlstrom, Leber's hereditary optic neuropathy and complex I deficiency in muscle, Ann. Neurol. 30 (1991) 701–708.
[11] A. Majander, K. Huoponen, M.L. Savontaus, E. Nikoskelainen, M. Wikstrom, Electron transfer properties of NADH:ubiquinone reductase in the ND1/3460 and the ND4/11778 mutations of the Leber hereditary optic neuroretinopathy (LHON), FEBS Lett. 292 (1991) 289–292.
[12] V. Carelli, A. Ghelli, M. Ratta, E. Bacchilega, S. Sangiorgi, R. Mancini, V. Leuzzi, P. Cortelli, P. Montagna, E. Lugaresi, M. Degli Esposti, Leber's hereditary optic neuropathy: biochemical effect of the 11778/ND4 and 3460/ND1 mutations and correlation with the mitochondrial genotype, Neurology 48 (1997) 1623–1632.
[13] H.R. Cock, J.M. Cooper, A.H.V. Schapira, Functional consequences of the 3460-bp mitochondrial DNA mutation associated with Leber's hereditary optic neuropathy, J. Neurol. Sci. 165 (1999) 10–17.
[14] M. Degli Esposti, V. Carelli, A. Ghelli, M. Ratta, M. Crimi, S. Sangiorgi, P. Montagna, G. Lenaz, E. Lugaresi, P. Cortelli, Functional alterations of the mitochondrially encoded ND4 subunit associated with Leber's hereditary optic neuropathy, FEBS Lett. 352 (1994) 375–379.
[15] L. Vergani, A. Martinuzzi, V. Carelli, P. Cortelli, P. Montagna, G. Schievano, R. Carrozzo, C. Angelini, E. Lugaresi, mtDNA mutations associated with Leber's hereditary optic neuropathy: studies on cytoplasmic hybrid (cybrid) cells, Biochem. Biophys. Res. Commun. 210 (1995) 880–888.
[16] G. Hofhaus, D.R. Johns, O. Hurko, G. Attardi, A. Chomyn, Respiration and growth defects in transmitochondrial cell lines carrying the 11778 mutation associated with Leber's hereditary optic neuropathy, J. Biol. Chem. 271 (1996) 13155–13161.
[17] M.D. Brown, I.A. Trounce, A.S. Jun, J.C. Allen, D.C. Wallace, Functional analysis of lymphoblast and cybrid mitochondria containing the 3460, 11778, or 14484 Leber's hereditary optic neuropathy mitochondrial DNA mutation, J. Biol. Chem. 275 (2000) 39831–39836.
[18] A. Baracca, G. Solaini, G. Sgarbi, G. Lenaz, A. Baruzzi, A.H. Schapira, A. Martinuzzi, V. Carelli, Severe impairment of complex I-driven adenosine triphosphate synthesis in Leber hereditary optic neuropathy cybrids, Arch. Neurol. 62 (2005) 730–736.
[19] V. Carelli, M. Rugolo, G. Sgarbi, A. Ghelli, C. Zanna, A. Baracca, G. Lenaz, E. Napoli, A. Martinuzzi, G. Solaini, Bioenergetics shapes cellular death pathways in Leber's hereditary optic neuropathy: a model of mitochondrial neurodegeneration, Biochim. Biophys. Acta 1658 (2004) 172–179.
[20] A. Wong, L. Cavelier, H.E. Collins-Schramm, M.F. Seldin, M. McGrogan, M.L. Savontaus, G.A. Cortopassi, Differentiation-specific effects of LHON mutations introduced into neuronal NT2 cells, Hum. Mol. Genet. 11 (2002) 431–438.
[21] A.P. Kudin, N.Y. Bimpong-Buta, S. Vielhaber, C.E. Elger, W.S. Kunz, Characterization of superoxide-producing sites in isolated brain mitochondria, J. Biol. Chem. 279 (2004) 4127–4135.
[22] C. Battisti, P. Formichi, E. Cardaioli, S. Bianchi, P. Mangiavacchi, S.A. Tripodi, P. Tosi, A. Federico, Cell response to oxidative stress induced apoptosis in patients with Leber's hereditary optic neuropathy, J. Neurol. Neurosurg. Psychiatry 75 (2004) 1731–1736.
[23] M. Floreani, E. Napoli, A. Martinuzzi, G. Pantano, V. De Riva, R. Trevisan, E. Bisetto, L. Valente, V. Carelli, F. Dabbeni-Sala, Antioxidant defences in cybrids harboring mtDNA mutations associated with Leber's hereditary optic neuropathy, FEBS J. 272 (2005) 1124–1135.
[24] S. Beretta, J.P.M. Wood, B. Derham, G. Sala, L. Tremolizzo, C. Ferrarese, N.N. Osborne, Partial mitochondrial complex I inhibition induces oxidative damage and perturbs glutamate transport in primary retinal cultures. Relevance to Leber Hereditary Optic Neuropathy (LHON), Neurobiol. Dis. 24 (2006) 308–317.
[25] S. DiMauro, M. Mancuso, Mitochondrial diseases: therapeutic approaches, Biosci. Rep. 27 (2007) 125–137.
[26] J. Guy, X. Qi, F. Palotti, E.A. Schon, G. Manfredi, V. Carelli, A. Martinuzzi, W.W. Hauswirth, A.S. Lewin, Rescue of a mitochondrial deficiency causing Leber hereditary optic neuropathy, Ann. Neurol. 52 (2002) 534–542.
[27] G. Manfredi, J. Fu, J. Ojaimi, J.E. Sallock, J.Q. Kwong, J. Guy, E.A. Schon, Rescue of a deficiency in ATP synthesis by transfer of MTATP6, a mitochondrial DNA-encoded gene to the nucleus, Nat. Genet. 30 (2002) 394–399.
[28] J. Oca-Cossio, L. Kenyon, H. Hao, C.T. Moraes, Limitations of allotopic expression of mitochondrial genes in mammalian cells, Genetics 165 (2003) 707–720.
[29] M. Bokori-Brown, I.J. Holt, Expression of Alga1 nuclear ATP synthase subunit 6 in human cells results in protein targeting to mitochondria but no assembly into ATP synthase, Rejuvenation Res. 9 (2006) 455–469.
[30] M.G. Claros, J. Perea, Y. Shu, F.A. Samatey, J.L. Popot, C. Jacq, Limitations to in vivo import of hydrophobic proteins into yeast mitochondria: the case of a cytoplasmic synthesized apocytochrome *b*, Eur. J. Biochem. 228 (1995) 762–771.
[31] P.M. Smith, G.F. Ross, R.W. Taylor, D.M. Turnbull, R.N. Lightowlers, Strategies for treating disorders of the mitochondrial genome, Biochem. Biophys. Acta 1659 (2004) 232–239.
[32] C. Bonnet, V. Kaltimbacher, S. Ellouze, S. Augustin, P. Benit, V. Forster, P. Rustin, J.A. Sahel, M. Corral-Debrinski, Allotopic mRNA localization to the mitochondrial surface rescues respiratory chain defects in fibroblasts harboring mitochondrial DNA mutations affecting complex I or V subunits, Rejuvenation Res. 10 (2007) 127–144.
[33] J. Sylvestre, A. Margeot, C. Jacq, G. Dujardin, M. Corral-Debrinski, The role of the 3′ UTR in mRNA sorting to the vicinity of mitochondria is conserved from yeast to human cells, Mol. Biol. Cell 14 (2003) 3848–3856.
[34] V. Kaltimbacher, C. Bonnet, G. Lecoeuvre, V. Forster, J.A. Sahel, M. Corral-Debrinski, mRNA localization to the mitochondrial surface allows the efficient translocation inside the organelle of a nuclear recoded ATP6 protein, RNA 12 (2006) 1408–1417.
[35] L.G. Nijtmans, N.S. Henderson, I.J. Holt, Blue Native electrophoresis to study mitochondrial and other protein complexes, Methods 26 (2002) 327–334.
[36] P. Benit, S. Goncalves, E.P. Dassa, J.J. Brière, G. Martin, P. Rustin, Three spectrophotometric assays for the measurement of the five respiratory chain complexes in minuscule biological samples, Clin. Chim. Acta 374 (2006) 81–86.
[37] P. Rustin, D. Chretien, T. Bourgeron, B. Gerard, A. Rotig, J.M. Saudubray, A. Munnich, Biochemical and molecular investigations in respiratory chain deficiencies, Clin. Chim. Acta 228 (1994) 35–51.
[38] A. Ghelli, C. Zanna, A.M. Porcelli, A.H. Schapira, A. Martinuzzi, V. Carelli, M. Rugolo, Leber's hereditary optic neuropathy (LHON) pathogenic mutations induce mitochondrial-dependent apoptotic death in transmitochondrial cells incubated with galactose medium, J. Biol. Chem. 278 (2003) 4145–4150.
[39] F. Pallotti, A. Baracca, E. Hernandez-Rosa, W.F. Walker, G. Solaini, G. Lenaz, G.V. Melzi D'Eril, S. Dimauro, E.A. Schon, M.M. Davidson, Biochemical analysis of respiratory function in cybrid cell lines harbouring mitochondrial DNA mutations, Biochem. J. 384 (2004) 287–293.
[40] R. McFarland, R.W. Taylor, D.M. Turnbull, Mitochondrial disease—its impact, etiology, and pathology, Curr. Top. Dev. Biol. 77 (2007) 113–155.
[41] K.K. Singh, Mitochondria damage checkpoint, aging, and cancer, Ann. N. Y. Acad. Sci 1067 (2006) 182–190.

[42] P.Y.W. Man, D.M. Turnbull, P.F. Chinnery, Leber hereditary optic neuropathy, J. Med. Genet. 39 (2002) 162–169.
[43] P. Rustin, D. Chretien, T. Bourgeron, A. Wucher, J.M. Saudubray, A. Rotig, A. Munnich, Assessment of the mitochondrial respiratory chain, Lancet 338 (1991) 60.
[44] W.J.H. Koopman, S. Verkaart, H.J. Visch, S. Van Emst-de Vries, L.G.J. Nijtmans, J.A.M. Smeitink, P.H.G.M. Willems, Human NADH:ubiquinone oxidoreductase deficiency: radical changes in mitochondrial morphology? Am. J. Physiol., Cell Physiol. 293 (2007) 22–29.
[45] M. Lazarou, M. McKenzie, A. Ohtake, D.R. Thorburn, M.T. Ryan, Analysis of the assembly profiles for mitochondrial- and nuclear-DNA-encoded subunits into complex I, Mol. Cell. Biol. 27 (2007) 4228–4237.
[46] R.O. Vogel, J.A.M. Smeitink, L.G.J. Nijtmans, Human mitochondrial complex I assembly: a dynamic and versatile process, Biochem. Biophys. Acta 1767 (2007) 1215–1227.
[47] X. Qi, L. Sun, A.S. Lewin, W.W. Hauswirth, J. Guy, The mutant human ND4 subunit of complex I induces optic neuropathy in the mouse, Invest. Ophthalmol. Vis. Sci. 48 (2007) 1–10.